On new $\mathfrak{V}$-line Radon transforms in $\mathbb{R}^2$ and their inversion

2011 J. Phys. A: Math. Theor. 44 075206

(http://iopscience.iop.org/1751-8121/44/7/075206)

IOP PUBLISHING JOURNAL OF PHYSICS A: MATHEMATICAL AND THEORETICAL

J. Phys. A: Math. Theor. **44** (2011) 075206 (13pp) doi:10.1088/1751-8113/44/7/075206

On new $\mathfrak{V}$-line Radon transforms in $\mathbb{R}^2$ and their inversion

T T Truong[1,3] **and M K Nguyen**[2]

[1] Laboratoire de Physique Théorique et Modélisation, (CNRS UMR 8089/Université de Cergy-Pontoise), 2 av. Adolphe Chauvin, 95302 Cergy-Pontoise, France
[2] Laboratoire Equipes Traitement de l'Information et Systèmes, (CNRS UMR 8051/ENSEA/Université de Cergy-Pontoise), 2 av. Adolphe Chauvin, 95302 Cergy-Pontoise, France

E-mail: truong@u-cergy.fr

Received 6 September 2010, in final form 8 December 2010
Published 28 January 2011
Online at stacks.iop.org/JPhysA/44/075206

Abstract

Radon transforms on piecewise smooth curves in $\mathbb{R}^2$ are rather unfamiliar and have not been so far widely investigated. In this paper we consider three types of Radon transforms defined on a pair of half-lines in the shape of a V, with a fixed axis direction. These three Radon transforms arise from recently suggested tomographic procedures. Our main result consists in obtaining their analytic inverse formulas, which may serve as mathematical foundation for new imaging systems in engineering and physics.

(Some figures in this article are in colour only in the electronic version)

1. Introduction

Radon transforms in the plane have been extensively studied in the past. Besides the cases of a straight line [1], and a circle intersecting a fixed point, Radon transforms on other classes of curves have also been treated (see among other works e.g. [2–4]). The universality of a Radon transform is known in imaging science ranging from medicine [5, 6], seismic [7], astrophysics [8], non-destructive industrial testing [9], etc. It also plays a crucial role in pure mathematics [10–13] and recently has become an increasingly powerful investigation tool in numerous fields of physics, e.g. [14–18].

In 1997 Basko introduced a Radon transform on a pair of half-lines forming a V-shape in an attempt to model image formation in the so-called one-dimensional Compton camera [19]. The axis of this $\mathfrak{V}$-line swings around a point of the plane such that its vertex lies on a straight line (representing a 'scattering' detector) and the opening angle of the two half-lines (representing a Compton scattering angle) is an imaging data variable. No other cases of

[3] Author to whom any correspondence should be addressed.

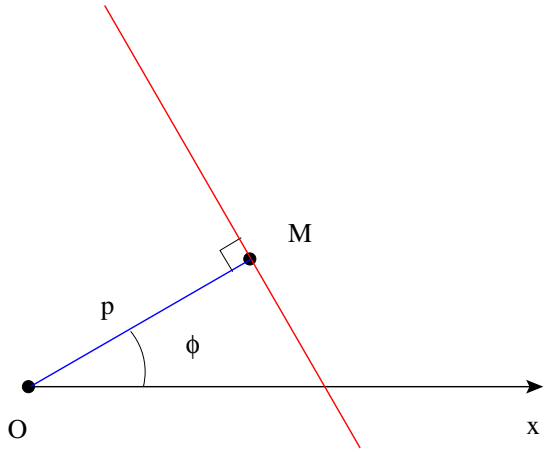

Figure 1. Parameters of the Radon transform.

Radon transforms on piecewise lines (or curves) seem to have been discussed in the literature until we recently put forward the idea of $\mathfrak{V}$-line Radon transforms with a fixed axis direction [20]. An concept akin to a broken ray Radon transform has recently appeared [21].

In this work we consider the class of $\mathfrak{V}$-line Radon transforms with a fixed symmetry axis direction. Such Radon transforms may be of theoretical interest in integral geometry in the sense of Gel'fand [11]. Three types of $\mathfrak{V}$-line Radon transforms with fixed axis direction will be treated. The first is mathematically the most important and arises from a coupled transmission–reflection tomographic process while the other two are its variants corresponding respectively to a collimated one-dimensional Compton camera and to scattered radiation emission imaging using a one-dimensional gamma camera. For all three cases an exact inverse formula is established. These results are of theoretical nature: they support the feasibility of three new tomographies. An illustration of these inversion formulas in two-dimensional medical and industrial imaging can be found in [20]. The paper closes with a short conclusion and some forthcoming topics of investigation.

2. The $\mathfrak{V}$-line Radon transform

2.1. Short review of the standard Radon transform

Before going into the subject, we briefly review the standard Radon transform. It maps an $L^1(\mathbb{R}^2)$-function $f(x, y)$ onto $\mathfrak{R}f(p, \phi)$ *via* the integral

$$\mathfrak{R}f(p, \phi) = \int_{\mathbb{R}^2} \mathrm{d}x\, \mathrm{d}y f(x, y)\delta(p - x\cos\phi - y\sin\phi),$$

in which p is the distance from the coordinate system origin to the straight line and ϕ is the angle of the normal unit vector to the line with the Ox-axis, see figure 1.

From the structure of the delta function kernel, it follows that

$$\mathfrak{R}f(p, \phi) = \mathfrak{R}f(-p, \phi + \pi).$$

There exists an explicit inverse formula [5]

$$f(x, y) = \frac{1}{2\pi^2} \int_0^\pi \mathrm{d}\phi \left(\text{P.V.} \int_{\mathbb{R}} \mathrm{d}p\, \frac{\mathfrak{R}'f(p, \phi)}{(p - x\cos\phi - y\sin\phi)}\right), \tag{1}$$

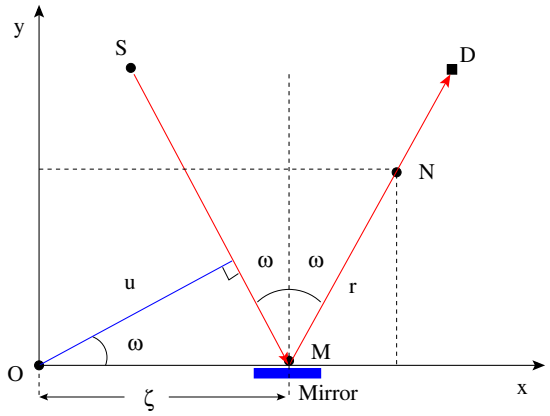

Figure 2. Parameters of the $\mathfrak{V}$-line Radon transform.

where

$$\mathfrak{R}' f(p, \phi) = \frac{\partial}{\partial p} \mathfrak{R} f(p, \phi).$$

In equation (1), the p-integral is a Cauchy principal value (P.V.). An alternative form in Fourier space of this inverse formula is

$$f(x, y) = \int_0^{\pi} \mathrm{d}\phi \int_{\mathbb{R}} \mathrm{d}k |k| \, \mathrm{e}^{2\mathrm{i}\pi k(x\cos\phi + y\sin\phi)} \int_{\mathbb{R}} \mathrm{d}q \, \mathrm{e}^{-2\mathrm{i}\pi qk} \mathfrak{R} f(q, \phi),$$

which expresses a summation image of the 'ramp'-filtered Radon data [5].

2.2. *Definition*

Consider a pair of half-lines meeting at a point **M** of abscissa ζ on the Ox-axis, each of which making an angle ω $(0 < \omega < \pi/2)$ with the Oy-axis, see figure 2. Let $f(x, y)$ be an $L^1(\mathbb{R}^2)$ non-negative continuous function with compact support in $\{\mathbb{R}^2 | y > 0\}$. We call

$$\mathfrak{V} f(\zeta, \tau) = \int_0^{\infty} \mathrm{d}r \ (f(\zeta + r\sin\omega, r\cos\omega) + f(\zeta - r\sin\omega, r\cos\omega)), \tag{2}$$

the $\mathfrak{V}$-line Radon transform of $f(x, y)$, where $\tau = \tan\omega$.

Equation (2) may be put under the form of an integral transform in $\mathbb{R}^2$ with a delta function kernel concentrated on the $\mathfrak{V}$-line

$$\mathfrak{V} f(\zeta, \tau) = \int_{\mathbb{R}^2} \mathrm{d}x \, \mathrm{d}y \mathcal{K}_{\mathfrak{V}}(\zeta, \omega | x, y) f(x, y),$$

with

$$\mathcal{K}_{\mathfrak{V}}(\zeta, \omega | x, y) = (\delta((x - \zeta)\cos\omega - y\sin\omega) + \delta((x - \zeta)\cos\omega + y\sin\omega)).$$

Thus the image of a given point source at $(x, y) \in \mathbb{R}^2$ is the sum of two Dirac delta distributions, which have a support in the upper (τ, ζ)-plane, consisting of two half-lines, with $\tau > 0$, meeting at $\xi = x$ on the ξ-axis and having a slope $\pm y^{-1}$, i.e.

$$\tau = \left| \frac{x - \zeta}{y} \right| \quad \text{or} \quad \omega = \arctan \left| \frac{x - \zeta}{y} \right|.$$

In a (ω, ζ)-representation, this is just the arctan-curve, which is the support of the point-source image. Thus the support of $\mathfrak{V}f(\zeta, \tau)$ is not compact in this representation.

Clearly the $\mathfrak{V}$-Radon transform can also be written in the language of the standard Radon transform as

$$\mathfrak{V}f(\zeta, \tau) = \int_{\mathbb{R}} \mathrm{d}x \int_0^\infty \mathrm{d}y f(x, y)(\delta(u - x\cos\omega - y\sin\omega) + \delta(u - x\cos\omega + y\sin\omega)),$$

where $u = \zeta\cos\omega$, the distance of the coordinate origin to the two half-lines forming the letter V. Note also that the unit normal vectors to these half-lines make an angle $\pm\omega$ with the Ox-axis. So the result appears as the sum of two standard Radon transforms of $f(x, y)$, except for the y-integration range.

2.3. Physical implementation

In standard computed tomography, a calibrated x-ray pencil emitted from a point-source **S** traverses a two-dimensional slice of an object along a straight line before being absorbed by a point-like detector **D**. In this way, the attenuation of the radiation beam is expressed as an integral of the linear attenuation function of the object to be imaged over a straight line. This is Radon's problem which is solved by equation (1).

The $\mathfrak{V}$-line Radon transform may be conceived as representing the measurement of an x-ray pencil attenuation along a broken path in the shape of a V, which is physically realized by putting a mirror at the vertex **M** of the $\mathfrak{V}$-line as shown in figure 2. Measurements requiring various angles ω may be performed by varying the distance SD, but in practice one may set a series of point-sources and a series of point-detectors respectively on the left and on the right of a given axis of symmetry of the $\mathfrak{V}$-line. To vary the parameter ζ, one may put the object on a conveyor belt in a scanning process. Such a device is clearly a new type of x-ray scanner which could prove to be more efficient wherever the rotational motion of a standard x-ray scanner cannot be used and should be replaced by a translational motion. Such a situation would arise when tomographic images of series of objects on a conveyor belt are to be taken successively. As possible applications, one may think of luggage control in airports as well as continuous imaging of series of biological objects in medical research.

2.4. Inversion formula

We now establish a relation between Radon transform and Fourier transform which is used to obtain the inverse of the $\mathfrak{V}$-line Radon transform. For the standard Radon transform, such a relation shows how this transform appears in Fourier spaces. It is known in imaging science as the central-slice theorem [5].

As $\mathfrak{V}$-lines of a given opening angle ω can be deduced from each other by x-translations, we may introduce the x-Fourier transform $\widetilde{f}(p, y)$ of $f(x, y)$ by

$$f(x, y) = \int_{-\infty}^{\infty} \mathrm{d}p\ \mathrm{e}^{2\mathrm{i}\pi px}\, \widetilde{f}(p, y).$$

Equation (2) can now be rewritten as

$$\mathfrak{V}f(\zeta, \tau) = \int_{-\infty}^{\infty} \mathrm{d}p\, \mathrm{e}^{2\mathrm{i}\pi p\zeta} \int_0^\infty \mathrm{d}r\, \widetilde{f}(p, r\cos\omega)\ 2\cos(2\pi pr\sin\omega). \tag{3}$$

To proceed further we set $z = r\cos\omega$. Recalling that $0 < \omega < \pi/2$, we have

$$z > 0 \quad \text{and} \quad \cos\omega = \frac{1}{\sqrt{1+\tau^2}} > 0.$$

Then equation (3) appears as

$$\mathfrak{V}f(\zeta,\tau) = 2\sqrt{1+\tau^2}\int_{-\infty}^{\infty} \mathrm{d}p\ \mathrm{e}^{2\mathrm{i}\pi p\zeta}\ \int_0^{\infty} \mathrm{d}z\ \widetilde{f}(p,z)\ \cos(2\pi p\tau z). \tag{4}$$

Extracting the p-Fourier component $\widetilde{\mathfrak{V}f}(p,\tau)$ of $\mathfrak{V}f(\zeta,\tau)$ on the left-hand side of equation (4) gives

$$\int_{\mathbb{R}} \mathrm{d}\zeta\ \mathrm{e}^{-2\mathrm{i}\pi\zeta p}\left(\frac{\mathfrak{V}f(\zeta,\tau)}{\sqrt{1+\tau^2}}\right) = 2\int_0^{\infty} \mathrm{d}z\widetilde{f}(p,z)\cos(2\pi p\tau z).$$

We now multiply both sides of this equation by $\cos(2\pi\tau v)$ and integrate on $\tau > 0$. Using the identity

$$\int_0^{\infty} \mathrm{d}\tau\ \cos(2\pi\tau\, v)\ \cos(2\pi k z\,\tau) = \frac{1}{4}\left(\delta(kz+v)+\delta(kz-v)\right), \tag{5}$$

we obtain

$$\int_0^{\infty} \mathrm{d}\tau\cos(2\pi\tau v)\int_{\mathrm{R}} \mathrm{d}\zeta\ \mathrm{e}^{-2\mathrm{i}\pi\zeta p}\left(\frac{\mathfrak{V}f(\zeta,\tau)}{\sqrt{1+\tau^2}}\right) = \frac{1}{2}\int_0^{\infty} \mathrm{d}z\widetilde{f}(p,z)(\delta(pz+v)+\delta(pz-v)),$$

with $(p,v)\in\mathbb{R}^2$ and $z>0$. We now perform the τ-integration:

- if $v/p>0$, then only $\delta(v-pz) = |p|^{-1}\delta(z-v/p)$ contributes,

$$\int_0^{\infty} \mathrm{d}\tau\cos(2\pi\tau v)\int_{\mathbb{R}} \mathrm{d}\zeta\ \mathrm{e}^{-2\mathrm{i}\pi\zeta p}\left(\frac{\mathfrak{V}f(\zeta,\tau)}{\sqrt{1+\tau^2}}\right) = \frac{1}{2|p|}\widetilde{f}(p,v/p);$$

- if $v/p<0$, then only $\delta(v+pz) = |p|^{-1}\delta(z+v/p)$ contributes,

$$\int_0^{\infty} \mathrm{d}\tau\cos(2\pi\tau v)\int_{\mathbb{R}} \mathrm{d}\zeta\ \mathrm{e}^{-2\mathrm{i}\pi\zeta p}\left(\frac{\mathfrak{V}f(\zeta,\tau)}{\sqrt{1+\tau^2}}\right) = \frac{1}{2|p|}\widetilde{f}(p,-v/p).$$

Hence we can regroup these two cases into a single formula as

$$\widetilde{f}(p,|v/p|) = 2|p|\int_0^{\infty} \mathrm{d}\tau\cos(2\pi\tau v)\int_{\mathbb{R}} \mathrm{d}\zeta\ \mathrm{e}^{-2\mathrm{i}\pi\zeta p}\left(\frac{\mathfrak{V}f(\zeta,\tau)}{\sqrt{1+\tau^2}}\right).$$

Putting $y = |v/p| > 0$, we can reconstruct $f(x,y)$ by an inverse Fourier transform in p and $f(x,y)$ is expressed as a triple integral on the $\mathfrak{V}$-line Radon data

$$f(x,y) = \int_{-\infty}^{\infty} |p|\ \mathrm{d}p\,\mathrm{e}^{2\mathrm{i}\pi px}\ \int_0^{\infty} \mathrm{d}\tau\ \frac{2\cos(2\pi p\tau y)}{\sqrt{1+\tau^2}}\ \int_{-\infty}^{\infty} \mathrm{d}\zeta\ \mathrm{e}^{-2\mathrm{i}\pi\zeta p}\ \mathfrak{V}f(\zeta,\tau), \tag{6}$$

where we have made use of the evenness of the cos-function.

Inspection of convergence shows that exchange of integration order is possible and equation (6) may now be rewritten as

$$f(x,y) = \int_0^{\infty}\frac{\mathrm{d}\tau}{\sqrt{1+\tau^2}}\int_{-\infty}^{\infty}|p|\,\mathrm{d}p\,\mathrm{e}^{2\mathrm{i}\pi px}(\mathrm{e}^{2\mathrm{i}\pi p\tau y}+\mathrm{e}^{-2\mathrm{i}\pi p\tau y})\int_{-\infty}^{\infty}\mathrm{d}\zeta\mathfrak{V}f(\zeta,\tau)\,\mathrm{e}^{-2\mathrm{i}\pi\zeta p}. \tag{7}$$

Thus analogously to the Radon transform, we can write

$$f(x,y) = \frac{1}{2\pi^2}\int_0^{\infty}\frac{\mathrm{d}\tau}{\sqrt{1+\tau^2}}\left(\mathrm{P.V.}\int_{\mathbb{R}}\mathrm{d}\zeta\ \left(\frac{\mathfrak{V}'f(\zeta,\tau)}{(\zeta-x-y\tau)}+\frac{\mathfrak{V}'f(\zeta,\tau)}{(\zeta-x+y\tau)}\right)\right), \tag{8}$$

where $\mathfrak{V}'f(\zeta,\tau)$ is the ζ-derivative of $\mathfrak{V}f(\zeta,\tau)$.

2.5. Alternative form of the inversion formula

Reintroducing $u = \zeta \cos\omega$, which is the common distance from the coordinate system origin to the two branches of the $\mathfrak{V}$-line, and redefining $f(\zeta, \tau)$ as $F(u, \omega)$, equation (8) becomes

$$f(x, y) = \frac{1}{2\pi^2} \int_0^{\pi/2} \mathrm{d}\omega \left(\mathrm{P.V.} \int_{\mathbb{R}} \mathrm{d}u \left[\frac{\mathfrak{V}' F(u, \omega)}{(u - x\cos\omega - y\sin\omega)} + \frac{\mathfrak{V}' F(u, \omega)}{(u - x\cos\omega + y\sin\omega)} \right] \right), \tag{9}$$

where $\mathfrak{V}' F(u, \omega)$ is the derivative of $\mathfrak{V} F(u, \omega)$ with respect to u. This expression is a sum of two ω-integrals which, as functions of (x, y) respectively, take a constant value along the half-line of the unit normal vector $\mathbf{n} = (\cos\omega, \sin\omega)$ and along the half-line of the unit normal vector $\mathbf{n}' = (\cos\omega, -\sin\omega)$. A similar feature occurs in the standard Radon transform but with a double angular range $[0, \pi]$. Thus we may view the $\mathfrak{V}$-line Radon transform as the sum of two half-line Radon $\mathfrak{R}$-transforms, as suggested by the defining equation (2). In imaging science, equation (9) is called a 'summation image' of back-projected Radon data [5], the ζ-derivative of the data being back-projected on the left and on the right branches of the $\mathfrak{V}$-line in the ζ-integrand of equation (9).

2.6. Extension to the range $\pi/2 < \omega < \pi$

Until now, we have considered $L_0^1(\mathbb{R}^2)$-functions with compact support. By appropriate translations, their support can be shifted into the upper half-plane. But when the support of $f(x, y)$ is extended over all $\mathbb{R}^2$, we need to collect data pertaining to the part of its support below the real axis. This can be achieved using the angular range $\pi/2 < \omega < \pi$, for which $\cos\omega$ and τ are negative. The $\mathfrak{V}$-line is now up-side down. In this case, we set $z = -z'$ and $\tau = -\tau'$ in equation (2.4) to have

$$\int_{\mathbb{R}} \mathrm{d}p\, \mathrm{e}^{-2\mathrm{i}\pi p\zeta} \left(\frac{\mathfrak{V} f(\zeta, -\tau')}{\sqrt{1 + \tau'^2}} \right) = 2 \int_0^{\infty} \mathrm{d}z' \widetilde{f}(p, -z') \cos(2\pi p z' \tau'),$$

since $z\tau = z'\tau'$, $\mathrm{d}z = -\mathrm{d}z'$ and because of $\cos\omega = -1/\sqrt{1 + \tau'^2}$. This shows that again we have to invert a cosine-Fourier transform to reconstruct $f(x, y)$ for $y < 0$. Following the previous steps we obtain

$$\int_0^{\infty} \mathrm{d}\tau' \cos(2\pi\tau' v) \int_{\mathbb{R}} \mathrm{d}\zeta\, \mathrm{e}^{-2\mathrm{i}\pi\zeta p} \left(\frac{\mathfrak{V} f(\zeta, -\tau')}{\sqrt{1 + \tau'^2}} \right) = \frac{1}{2} \int_0^{\infty} \mathrm{d}z' \widetilde{f}(p, -z')(\delta(pz' + v) + \delta(pz' - v)),$$

with $(p, v) \in \mathbb{R}^2$ and $z' > 0$. We now perform the z'-integration on the right-hand side of this last equation;

- if $v/p > 0$, then only $\delta(v - pz') = |p|^{-1}\delta(z' - v/p)$ contributes,

$$\int_0^{\infty} \mathrm{d}\tau' \cos(2\pi\tau' v) \int_{\mathbb{R}} \mathrm{d}\zeta\, \mathrm{e}^{-2\mathrm{i}\pi\zeta p} \left(\frac{\mathfrak{V} f(\zeta, -\tau')}{\sqrt{1 + \tau'^2}} \right) = \frac{1}{2|p|} \widetilde{f}(p, -v/p);$$

- if $v/p < 0$, then only $\delta(v + pz') = |p|^{-1}\delta(z' + v/p)$ contributes,

$$\int_0^{\infty} \mathrm{d}\tau' \cos(2\pi\tau' v) \int_{\mathbb{R}} \mathrm{d}\zeta\, \mathrm{e}^{-2\mathrm{i}\pi\zeta p} \left(\frac{\mathfrak{V} f(\zeta, -\tau')}{\sqrt{1 + \tau'^2}} \right) = \frac{1}{2|p|} \widetilde{f}(p, v/p).$$

Analogously to the case with $0 < \omega < \pi/2$ (see equation (6)), we can write a single formula

$$\widetilde{f}(p, -|v/p|) = 2|p| \int_0^\infty \mathrm{d}\tau' \cos(2\pi\tau' v) \int_{\mathbb{R}} \mathrm{d}\zeta\, \mathrm{e}^{-2\mathrm{i}\pi\zeta p} \left(\frac{\mathfrak{V} f(\zeta, -\tau')}{\sqrt{1+\tau'^2}} \right).$$

Putting $y = -|v/p| > 0$, we can reconstruct $f(x, y)$ by the inverse Fourier transform in p for $y < 0$. Using again the evenness of the cos-function, $f(x, y)$ is then expressed as a triple integral on the $\mathfrak{V}$-line Radon data

$$f(x, y) = \int_{-\infty}^{\infty} |p|\, \mathrm{d}p\, \mathrm{e}^{2\mathrm{i}\pi p x} \int_0^\infty \mathrm{d}\tau' \frac{2\cos(2\pi p\tau' y)}{\sqrt{1+\tau'^2}} \int_{-\infty}^{\infty} \mathrm{d}\zeta\, \mathrm{e}^{-2\mathrm{i}\pi\zeta p} \mathfrak{V} f(\zeta, -\tau').$$

And hence for $y < 0$, we obtain

$$f(x, y) = \frac{-1}{2\pi^2} \int_0^\infty \frac{\mathrm{d}\tau'}{\sqrt{1+\tau'^2}}\, \mathrm{P.V.} \left(\int_{\mathbb{R}} \mathrm{d}\zeta \left(\frac{\mathfrak{V}' f(\zeta, -\tau')}{(x + \tau' y - \zeta)} + \frac{\mathfrak{V}' f(\zeta, -\tau')}{(x - \tau' y - \zeta)} \right) \right). \tag{10}$$

To sum up, formulas (8) give the reconstruction of a function $f(x, y)$ with compact support, which can always be, by an appropriate choice of the coordinate origin, positioned in the upper half-plane ($y > 0$). But when the support of $f(x, y)$ is infinitely extended and $f(x, y)$ decreases fast at infinity, the reconstruction formula (10) for ($y < 0$) should be used. We can put (8) and (10) together in one single formula as

$$f(x, y) = \frac{-1}{2\pi^2} \int_0^\infty \frac{\mathrm{d}\sigma}{\sqrt{1+\sigma^2}} \mathrm{P.V.} \left(\int_{\mathbb{R}} \mathrm{d}\zeta \left(\frac{\mathfrak{V}' f(\zeta, (\mathrm{sgn} y)\sigma)}{(x + \sigma y - \zeta)} + \frac{\mathfrak{V}' f(\zeta, (\mathrm{sgn} y)\sigma)}{(x - \sigma y - \zeta)} \right) \right),$$

where $(\mathrm{sgn} y)$ is the sign of y. This completes the proof of the inversion of the $\mathfrak{V}$-line Radon transform with fixed axis direction for all values of $y \in \mathbb{R}$.

2.7. Adjoint transform

The kernel $\mathcal{K}_{\mathfrak{V}}(\zeta, \omega | x, y)$ may be used to define an adjoint $\mathfrak{V}$-line Radon transform $\mathfrak{V}^+$. For an integrable function $g(\zeta, \omega)$, $\mathfrak{V}^+ g(x, y)$ is given by

$$\mathfrak{V}^+ g(x, y) = \int_0^{\pi/2} \mathrm{d}\omega \int_{\mathbb{R}} \mathrm{d}\zeta\, \mathcal{K}_{\mathfrak{V}}(\zeta, \omega | x, y) g(\zeta, \omega).$$

After performing the ζ-integration, the following form appears:

$$\mathfrak{V}^+ g(x, y) = \int_0^{\pi/2} \frac{\mathrm{d}\omega}{\cos\omega} \left(g(x - y\tau, \omega) + g(x + y\tau, \omega) \right),$$

where $\tau = \tan\omega$ as before. We observe that $g(x - y\tau, \omega)$ is constant on the left half-line of equation $(y - y_0)\tau = (x - x_0)$, whereas $g(x + y\tau, \omega)$ is constant on the right half-line of equation $-(y - y_0)\tau = (x - x_0)$.

The inverse formula of equation (8) has been viewed already as a 'summation image' of back-projected $\mathfrak{V}$-line Radon data (see equation (9)). Here it may be now viewed as the $\mathfrak{V}$-line adjoint Radon transform of the data with the identifications

$$\int_0^\infty \frac{\mathrm{d}\tau}{\sqrt{1+\tau^2}} = \int_0^{\pi/2} \mathrm{d}\omega,$$

and

$$g(x - y\tau, \omega) = \mathrm{P.V.} \frac{1}{2\pi^2} \int_{\mathbb{R}} \mathrm{d}\zeta \frac{\mathfrak{V}' f(\zeta, \tau)}{(\zeta - x + y\tau)},$$

$$g(x + y\tau, \omega) = \mathrm{P.V.} \frac{1}{2\pi^2} \int_{\mathbb{R}} \mathrm{d}\zeta \frac{\mathfrak{V}' f(\zeta, \tau)}{(\zeta - x - y\tau)}.$$

This behavior also shows up in the standard Radon transform [5].

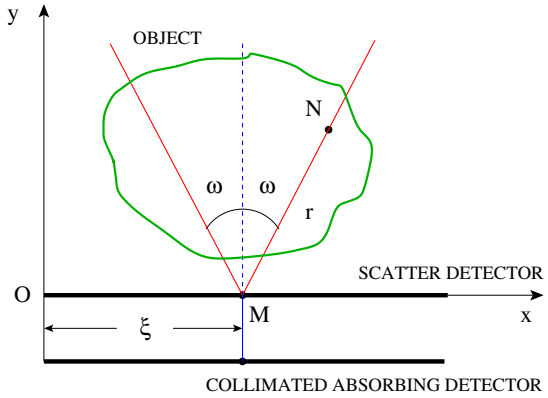

Figure 3. The $\mathfrak{V}^*$-line Radon transform and its parameters.

3. The $\mathfrak{V}^*$-line Radon transform

3.1. Definition

A variant of the $\mathfrak{V}$-line Radon transform arises when the integration measure on the half-lines is performed with a non-uniform density along the branches of the $\mathfrak{V}$-line.

Technically this occurs in the so-called one-dimensional special Compton camera for flat radiating objects [20], which is a special version of an imaging device investigated by [22] in three dimensions, see figure 3. Here a radiation-emitting object is described by its radioactivity emission density $f(x, y)$. Emitted radiation from a point-source **N** will Compton scatter electric charges, under a scattering angle ω, in the scatter detector before entering a collimated absorbing detector. The amount of scattered gamma radiation detected is thus given by the $\mathfrak{V}^*$-line Radon transform of $f(x, y)$, over an integration measure $m_\sigma(r)$, which accounts for radiation dispersion from object emission site to scattering site on the scatter detector. Upon close analysis, the integration measure is given by the two-dimensional photometric law as

$$m_\sigma(r) = \frac{1}{\pi\sigma} \tan^{-1} \frac{\sigma}{2r},$$

where σ is the linear size of scatterers. As in the previous section, we assume that the support of $f(x, y)$ is strictly in the upper half-plane $y > 0$. To keep the discussion simple and concentrate on the nature of this transform, we have ignored the Compton kinematic factor, which includes the Klein–Nishina scattering probability density.

Thus this alternate $\mathfrak{V}^*$-line Radon transform, for $f(x, y) \in L^1_0\left(\mathbb{R}^2_+\right)$, (functions with compact support in $\{\mathbb{R}^2 | y > 0\}$) has the form

$$\mathfrak{V}^* f(\zeta, \tau) = \int_0^\infty \mathrm{d}r m_\sigma(r) \left(f(\zeta + r\sin\omega, r\cos\omega) + f(\zeta - r\sin\omega, r\cos\omega)\right).$$

For $\sigma \neq 0$, an inversion formula cannot be worked out at present. But for vanishingly small target size $\sigma \to 0$, it has a simpler form

$$\mathfrak{V}^* f(\zeta, \tau) = \int_0^\infty \frac{\mathrm{d}r}{2\pi r} (f(\zeta + r\sin\omega, r\cos\omega) + f(\zeta - r\sin\omega, r\cos\omega)), \tag{11}$$

which can be inverted with the procedure of section 2. Since the support of f is 'above' the Ox-axis, the integral in equation (11) is well defined.

The integral kernel has the form

$$\mathcal{K}_{\mathfrak{V}^*}(\zeta, \omega|x, y) = \frac{1}{2\pi y}\left(\delta((x-\zeta)\cos\omega - y\sin\omega) + \delta((x-\zeta)\cos\omega + y\sin\omega)\right).$$

It differs from the kernel $\mathcal{K}_{\mathfrak{V}}(\zeta, \omega|x, y)$ by a factor $1/2\pi y$ due to the presence of $1/2\pi r$ in the r-integration. Its support is the same as the one given by equation (2.2).

3.2. Inversion formula

We follow now the steps and use the same notations as before. Equation (11) becomes

$$\int_{\mathbb{R}} \mathrm{d}\zeta\, \mathrm{e}^{-2\mathrm{i}\pi\zeta p}\mathfrak{V}^* f(\zeta, \tau) = \frac{1}{\pi}\int_0^\infty \mathrm{d}z \left(\frac{1}{z}\widetilde{f}(p, z)\right)\cos(2\pi\tau p z).$$

We now apply on both sides of this equation the integral operator

$$\int_0^\infty \mathrm{d}\tau\, \cos(2\pi\tau v),$$

and use the identity (5) to have

$$\int_0^\infty \mathrm{d}\tau\, \cos(2\pi\tau v)\int_{\mathbb{R}} \mathrm{d}\zeta\, \mathrm{e}^{-2\mathrm{i}\pi\zeta p}\mathfrak{V}^* f(\zeta, \tau) = \int_0^\infty \frac{\mathrm{d}z}{2\pi z}\widetilde{f}(p, z)\frac{1}{2}\left(\delta(v + pz) + \delta(v - pz)\right).$$

As $(p, v) \in \mathbb{R}^2$ and $z > 0$, there are two types of contributions:

- if $p\,v > 0$, only $\delta(v - pz) = |p|^{-1}\,\delta(z - v/p)$ contributes; hence,

  $$\int_0^\infty \frac{\mathrm{d}z}{2\pi z}\widetilde{f}(p, z)\frac{1}{2|p|}\delta\left(z - \frac{v}{p}\right) = \frac{1}{4\pi v}\mathrm{sgn}(p)\widetilde{f}\left(p, \frac{v}{p}\right) = \frac{\widetilde{f}\left(p, \frac{v}{p}\right)}{4\pi|v|},$$

  since $\mathrm{sgn}\,p = \mathrm{sgn}\,v$.
- if $p\,v < 0$, only $\delta(v + pz) = |p|^{-1}\,\delta(z + v/p)$ contributes; hence,

  $$\int_0^\infty \frac{\mathrm{d}z}{2\pi z}\widetilde{f}(p, z)\frac{1}{2|p|}\delta\left(z + \frac{v}{p}\right) = \frac{1}{2|p|}\frac{1}{2\pi\left(-\frac{v}{p}\right)}\widetilde{f}\left(p, -\frac{v}{p}\right) = \frac{\widetilde{f}\left(p, -\frac{v}{p}\right)}{4\pi|v|},$$

  since

  $$|p|\left(-\frac{v}{p}\right) = \mathrm{sgn}(p)(-1)|v|\mathrm{sgn}(v) = |v|,$$

  because $p\,v < 0$.

  We can put these two cases together with $y = |v/p|$ to have

  $$\widetilde{f}(p, |v/p|) = 2\pi|v|\int_0^\infty \mathrm{d}\tau\; 2\cos(2\pi\tau v)\int_{\mathbb{R}} \mathrm{d}\zeta\, \mathrm{e}^{-2\mathrm{i}\pi\zeta p}\;\mathfrak{V}^* f(\zeta, \tau). \qquad (12)$$

The reconstruction formula is then for $y = |v/p| > 0$, thanks to the evenness of the cos-function

$$f(x, y) = 2\pi y\int_{\mathbb{R}} \mathrm{d}p\,|p|\,\mathrm{e}^{2\mathrm{i}\pi x}\int_0^\infty \mathrm{d}\tau\, 2\cos(2\pi\tau y\, p)\int_{\mathbb{R}} \mathrm{d}\zeta\, \mathrm{e}^{-2\mathrm{i}\pi\zeta p}\,\mathfrak{V}^* f(\zeta, \tau).$$

It can be rewritten also as a Barrett 'summation image' as

$$f(x, y) = 2\pi y\int_0^\infty \mathrm{d}\tau\int_{\mathbb{R}} \mathrm{d}p|p|\,\mathrm{e}^{2\mathrm{i}\pi x}(\mathrm{e}^{2\mathrm{i}\pi p y\tau} + \mathrm{e}^{-2\mathrm{i}\pi p y\tau})\int_{\mathbb{R}} \mathrm{d}\zeta\mathfrak{V}^* f(\zeta, \tau)\,\mathrm{e}^{-2\mathrm{i}\pi\zeta p}.$$

The p-integration is the same as in equation (7) and yields

$$f(x, y) = \frac{y}{\pi}\int_0^\infty \mathrm{d}\tau\;\left(\mathrm{P.V.}\int_{\mathbb{R}} \mathrm{d}\zeta\left(\frac{\mathfrak{V}'^* f(\zeta, \tau)}{(\zeta - x - y\tau)} + \frac{\mathfrak{V}'^* f(\zeta, \tau)}{(\zeta - x + y\tau)}\right)\right),$$

where $\mathfrak{V}'^* f(\zeta, \tau)$ is the ζ-derivative of $\mathfrak{V}^* f(\zeta, \tau)$.

This expression can also be represented as a summation image on back-projected data on a $\mathfrak{V}$-line in (x, y)-space, with $f(\zeta, \tau) = F(u, \omega)$

$$f(x, y) = \frac{y}{\pi} \int_0^{\pi/2} \frac{\mathrm{d}\omega}{\cos\omega} \mathrm{P.V.} \int_{\mathbb{R}} \mathrm{d}u \left[\frac{\mathfrak{V}'^* F(u, \omega)}{(u - x\cos\omega - y\sin\omega)} + \frac{\mathfrak{V}'^* F(u, \omega)}{(u - x\cos\omega + y\sin\omega)} \right]. \tag{13}$$

Note that the apparent singularity in the angular integration at $\omega = \pi/2$ does not exist thanks to the assumption on the support of $f(x, y)$.

3.3. Extension to the range $\pi/2 < \omega < \pi$

Repeating the approach of subsection 2.5, we obtain the complement of equation (12)

$$\widetilde{f}(p, -|v/p|) = 2\pi|v| \int_0^{\infty} \mathrm{d}\tau' 2\cos(2\pi\tau' v) \int_{\mathbb{R}} \mathrm{d}\zeta\, \mathrm{e}^{-2\mathrm{i}\pi\zeta p} \mathfrak{V}^* f(\zeta, -\tau'),$$

and the corresponding reconstruction formula for $y = -|v/p| < 0$:

$$f(x, y) = 2\pi y \int_{\mathbb{R}} \mathrm{d}p\, |p|\, \mathrm{e}^{2\mathrm{i}\pi x} \int_0^{\infty} \mathrm{d}\tau'\, 2\cos(2\pi\tau' y\, p) \int_{\mathbb{R}} \mathrm{d}\zeta\ \mathrm{e}^{-2\mathrm{i}\pi\zeta p}\, \mathfrak{V}^* f(\zeta, -\tau'),$$

or

$$f(x, y) = \left(\frac{y}{\pi}\right) \int_0^{\infty} \mathrm{d}\tau' \left(\mathrm{P.V.} \int_{\mathbb{R}} \mathrm{d}\zeta \left(\frac{\mathfrak{V}'^* f(\zeta, -\tau')}{(\zeta - x - y\tau')} + \frac{\mathfrak{V}'^* f(\zeta, -\tau')}{(\zeta - x + y\tau')} \right) \right). \tag{14}$$

Formula (13) gives the reconstruction of $f(x, y)$ when its support is compact for $y > 0$ and when it is not compact one must add (14). Note that these formulas differ from those of the $\mathfrak{V}$-transform. We can put (3.2) and (14) together in a single formula as

$$f(x, y) = \left(\frac{y}{\pi}\right) \int_0^{\infty} \mathrm{d}\sigma \left(\mathrm{P.V.} \int_{\mathbb{R}} \mathrm{d}\zeta \left(\frac{\mathfrak{V}'^* f(\zeta, (\mathrm{sgn}y)\sigma)}{(\zeta - x - y\sigma)} + \frac{\mathfrak{V}'^* f(\zeta, (\mathrm{sgn}y)\sigma)}{(\zeta - x + y\sigma)} \right) \right),$$

where $(\mathrm{sgn}y)$ is the sign of y. This completes the inversion of the $\mathfrak{V}^*$-line Radon transform by a factor y/π and by the form of the τ-integration. An interpretation of equation (14) in terms of back-projected data or in terms of its adjoint transform can also be made along the lines of the previous section.

4. The $\mathfrak{V}^\sharp$-line Radon transform

A third version of the $\mathfrak{V}$-line Radon transform is a so-called compounded or integrated form of the $\mathfrak{V}^*$-Radon transform over a given integration measure. It arises in scattered radiation emission imaging, a concept which has been extensively investigated in recent years [23–26]. If the Compton camera exploits the scattering of object-emitted radiation by an external scatterer in the form of a scatter detector for imaging purpose, this time it is the object itself (in fact its electric charges) which serves as natural scatterer. Thus the outgoing radiation from the object itself is registered now by a motionless collimated gamma camera (as opposed to a moving collimated linear detector as in single photon emission tomography (or SPECT)). The data are collected at various values of the scattering energies—or equivalently at various values of the scattering angles ω—see figure 4. Hence the detected radiation flux density appears as the $\mathfrak{V}^\sharp$-line Radon transform of the object radioactivity emission density $f(x, y)$, i.e.

$$\mathfrak{V}^\sharp f(\zeta, \tau) = \int_0^{\infty} \mathrm{d}\eta \left(\frac{1}{\pi\sigma'} \tan^{-1} \frac{\sigma'}{2\eta} \right) \int_0^{\infty} \mathrm{d}r \left(\frac{1}{\pi\sigma} \tan^{-1} \frac{\sigma}{2r} \right)$$
$$\times [f(\zeta + r\sin\omega, \eta + r\cos\omega) + f(\zeta - r\sin\omega, \eta + r\cos\omega)], \tag{15}$$

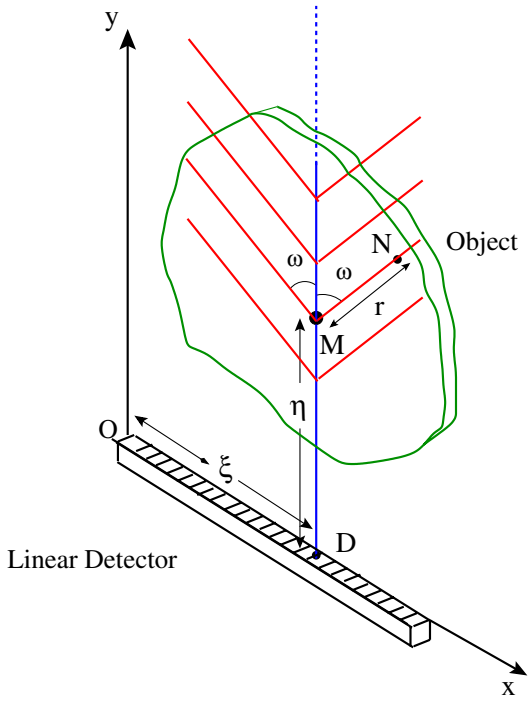

Figure 4. Setup and parameters of the $\mathfrak{V}^\sharp$-line Radon transform.

where σ' has the same meaning as in subsection 3.1[4]. A successful inversion of this $\mathfrak{V}^\sharp$-line Radon transform would allow us to reconstruct the radio-activity emission density $f(x, y)$ with a stationary linear collimated detector collecting series of 'images' at different scattering angles ω. This imaging process presents a very important advantage over the existing ones: it avoids the motion of the detector around the object during data acquisition, hence does not require the heavy bulky rotational mechanics to be included.

This type of $\mathfrak{V}$-line transform is called 'compounded' $\mathfrak{V}$-line Radon transform or $\mathfrak{V}^\sharp$-line Radon transform, by analogy to the three-dimensional case [23]. Now let us define

$$\int_0^\infty \mathrm{d}\eta \left(\frac{1}{\pi\sigma'} \tan^{-1}\frac{\sigma'}{2\eta}\right) f(\xi_\pm, \eta + r\cos\omega) = h(\xi_\pm, r\cos\omega), \tag{16}$$

where $\xi_\pm = (\zeta \pm r\sin\omega)$. Then we see that

$$\mathfrak{V}^\sharp f(\zeta, \tau) = \mathfrak{V}^* h(\zeta, \tau).$$

Hence the inversion problem is that of $\mathfrak{V}^*$ for h, followed by the extraction of f from equation (16).

Equation (15) may be rewritten as an integral transform with the kernel

$$\begin{aligned}\mathcal{K}_{\mathfrak{V}^\sharp}(\zeta, \tau|x, y) = \sqrt{1+\tau^2}\,(&Y(x-\zeta)Y(y-\tau(x-\zeta))m_\sigma((x-\zeta)\sqrt{1+\tau^2})m_{\sigma'}(y-\tau(x-\zeta))\\ &+ Y(-x+\zeta)Y(y+\tau(x-\zeta))m_\sigma(-(x-\zeta)\sqrt{1+\tau^2})m_{\sigma'}(y+\tau(x-\zeta))),\end{aligned}$$

where $Y(x)$ is the Heaviside unit step function. Here the kernel is not a Dirac delta function.

[4] Here also, for simplicity all technical pre-factors, e.g. the Klein–Nishina scattering probability in Compton effect, are discarded.

Section 3 shows how to reconstruct $h(x, y)$ from the data $\mathfrak{V}^\sharp f(\zeta, \tau)$ for all $(x, y) \in \mathbb{R}^2$. Thus given $h(x, y)$, f is the solution of the convolution equation

$$h(x, y) = \int_0^\infty \mathrm{d}\eta\, m_\sigma(\eta)\, f(x, \eta + y). \tag{17}$$

Let

$$f(x, y) = \int_{\mathbb{R}} \mathrm{d}k\, \mathrm{e}^{2\mathrm{i}\pi k y}\, \overline{f}(x, k) \quad \text{and} \quad \overline{m}_\sigma(k) = \int_0^\infty \mathrm{d}\eta\, \mathrm{e}^{2\mathrm{i}\pi k\eta} m_\sigma(\eta).$$

Then equation (17) becomes

$$h(x, y) = \int_{\mathbb{R}} \mathrm{d}k\, \mathrm{e}^{2\mathrm{i}\pi k y}\, \overline{f}(x, k)\, \overline{m}_\sigma(k).$$

Hence

$$\overline{f}(x, q) = \frac{1}{\overline{m}_\sigma(q)} \int_{\mathbb{R}} \mathrm{d}z\, \mathrm{e}^{-2\mathrm{i}\pi z q} h(x, z).$$

The recovery of $f(x, y)$ is achieved by the inverse Fourier transform

$$f(x, y) = \int_{\mathbb{R}} \mathrm{d}q\ \mathrm{e}^{2\mathrm{i}\pi q y}\, \frac{1}{\overline{m}_\sigma(q)} \int_{\mathbb{R}} \mathrm{d}z\, \mathrm{e}^{-2\mathrm{i}\pi z q}\, h(x, z), \tag{18}$$

as $h(x, z)$ is known for all $z \in \mathbb{R}$. As an example, in the limit $\sigma \to 0$, using the Fourier table [27], we have an exact expression for

$$\overline{m}_\sigma(q) = -\left(\ln 2\pi |q| - \gamma + \mathrm{i}\frac{\pi}{2}\operatorname{sgn} q\right)$$

to be substituted in equation (18) to reconstruct $f(x, y)$. We observe that the inversion of $\mathfrak{V}^\sharp$ is the product of the inversion of $\mathfrak{V}^\star$ times an inverse Fourier transform.

5. Conclusion and perspectives

In this paper we have presented for the first time three types of Radon transforms in $\mathbb{R}^2$ which are defined on a piecewise continuous curve having the shape of a letter V with a fixed axis direction. The main theoretical result is their analytic inverse formulas. These transforms are instrumental in new possible tomographic processes involving scattering, coupled transmission–reflection and emission phenomena. Numerical simulations on test phantoms to ascertain the viability of these imaging processes will appear in a separate publication.

We also envisage studying Radon transforms on more general piecewise continuous curves consisting of connected pieces of arcs, e.g. arcs of a circle, as well as Radon transforms on $\mathfrak{V}$-line with an axis swinging around a fixed point. Their inversion would open the way to new advantageous imaging processes. These topics are the object of future research.

References

[1] Radon J 1917 Über die Bestimmung von Funktionnen durch ihre Integralwerte längs gewisser Mannigfaltikeiten *Ber. Verh. Sachs. Akad. Wiss. Leipzig-Math.-Natur. Kl.* **69** 262–77

[2] Cormack A M 1983 The Radon transform on a family of curves in the plane *Proc. Am. Math. Soc.* **83** 325–30

[3] Quinto E T 1994 Radon transforms on curves in the plane *Tomography, Impedance Imaging and Integral Geometry (Lectures in Applied Mathematics* vol 30) (Providence, RI: American Mathematical Society) pp 231–44

[4] Nguyen M K and Truong T T 2010 Inversion of a new circular-arc Radon transform for Compton scattering tomography *Inverse Problems* **26** 065005

[5] Barrett H H 1984 The Radon transform and its applications *Progress in Optics* vol 21 ed E Wolf (Amsterdam: North-Holland) pp 219–86
[6] Natterer F 1986 *The Mathematics of Computerized Tomography* (New York: Wiley)
[7] Chapman C H 1981 Generalized Radon transforms and slant stacks *Geophys. J. R. Astron. Soc.* **66** 445–53
[8] Bracewell R N 1956 Strip integration in radio astronomy *Austr. J. Phys.* **9** 198–217
[9] Kershaw D 1970 The determination of the density distribution of a gas flowing in a pipe from mean density measurements *J. Inst. Math. Appl.* **6** 111–4
[10] John F 1955 *Planes Waves and Spherical Waves Applied to Partial Differential Equations* (New York: Interscience)
[11] Gelfand I M 1960 Integral geometry and its relations to the theory of group representation *Russ. Math. Surv.* **15** 143–51
[12] Militello B, Man'ko V I, Man'ko M A and Messina A 2009 Radon transform as a set of probability distributions *Phys. Scr.* **80** 058102
[13] Saygili K 2010 Trkalian fields and Radon transformation *J. Math. Phys.* **51** 033513
[14] Manuel A A 1982 Construction of the Fermi surface from positron-annihilation methods *Phys. Rev. Lett.* **49** 1525–8
[15] Behringer D *et al* 1982 A demonstration of ocean acoustic tomography *Nature* **229** 121–5
[16] Mane V, Peggs S and Wei J 1997 Radon reconstruction in longitudinal phase space *Proc. Particle Accelerator Conf. (Vancouver, BC, Canada, 12–16 May 1997)* vol 2, pp 2158–60
[17] Asorey M, Facchi P, Man'ko V I, Marmo G, Pascazio S and Sudarshan E G C 2007 Radon transform on the cylinder and tomography of a particle on the circle *Phys. Rev.* A **76** 012117
[18] Florescu L, Schotland J C and Markel V A 2009 Single scattering optical tomography *Phys. Rev.* E **79** 036607
[19] Basko R, Zeng G L and Gullberg G T 1997 Analytical reconstruction formula for the one-dimensional Compton camera *IEEE Trans. Nucl. Sci.* **44** 1342–46
[20] Morvidone M, Nguyen M K, Truong T T and Zaidi H 2010 On the V-line Radon transform and its imaging applications *Int. J. Biomed. Imaging* **2010** 208179
[21] Florescu L, Markel V A and Schotland J C 2010 Inversion formulas for the broken-ray Radon transform arXiv:1007.4183vl[math-phys]
[22] Cree M J and Bones P J 1994 Towards direct reconstruction from a gamma camera based on Compton scattering *IEEE Trans. Med. Imaging* **13** 398–407
[23] Nguyen M K and Truong T T 2002 On an integral transform and its inverse in nuclear imaging *Inverse Problems* **18** 265–77
[24] Nguyen M K, Truong T T and Grangeat P 2005 Radon transforms on a class of cones with fixed axis direction *J. Phys. A: Math. Gen.* **38** 8003–15
[25] Nguyen M K, Truong T T, Driol C and Zaidi H 2009 On a novel approach to Compton scattered emission imaging *IEEE Trans. Nucl. Sci.* **56** 1430–7
[26] Truong T T and Nguyen M K 2008 On a class of generalized Radon transform and its role in imaging science *Int. J. Pure Appl. Math.* **49** 373–80
[27] Lavoine J 1963 *Transformation de Fourier des Pseudo fonctions avec Tables de Nouvelles Transformées* (Paris: CNRS)